JOURNAL OF APPLIED ELECTROCHEMISTRY 26 (1996) 939–946

Influence of molybdenum on the anodic dissolution of iron in acidic solutions

M. BOJINOV, I. BETOVA

Central Laboratory of Electrochemical Power Sources, Bulgarian Academy of Sciences, 1113 Sofia, Bulgaria

R. RAICHEFF

Department of Electrochemical Technology and Corrosion Protection, Higher Institute of Chemical Technology, 1756 Sofia, Bulgaria

Received 10 October 1995; revised 20 January 1996

The anodic dissolution of pure iron and binary iron-molybdenum alloys (10 and 20 wt % Mo) in molar H_2SO_4 and HCl solutions was studied by d.c. polarization and a.c. impedance techniques. Molybdenum additive influences both the steady state polarization curves and the impedance spectra in the two media, the impact being stronger for the Fe–20 wt % Mo alloy. In general, two-slope polarization curves are obtained for the alloys; impedance spectra exhibit two time constants in addition to the charge transfer one implying the existence of two reaction intermediates. Differences between spectra measured in H_2SO_4 and HCl are discussed. A kinetic model advanced on the basis of literature data for pure iron and molybdenum was able to reproduce quantitatively both the steady state and a.c. impedance results for both alloys in the two media. Kinetic parameters for the anodic dissolution of Fe–Mo alloys are thereby determined.

1. Introduction

Molybdenum additive to stainless steels is known to improve resistivity to localized corrosive attack in media containing aggressive anions. Although the general cause of localized corrosion is believed to be the rupture of the passive film on the metal surface, no quantitative mechanism of this process has been advanced. Several years ago, MacDonald *et al.* [1–6] proposed the so-called point defect model (PDM) for the growth and chemical breakdown of passive films on metals. Based on this model, an approach to the mechanism of the influence of minor alloying elements on the susceptibility of stainless steels to localized attack was attempted (SVIM, solute-vacancy interaction model [7, 8]).

To collect more information for the electrochemical behaviour of an alloy, it is useful to study the pure metal constituents. The electrochemistry of iron in acidic media has been extensively studied. A quantitative model of its anodic dissolution in sulphate media (pH 0–5) featuring three reaction paths and four intermediate species was advanced by Keddam *et al.* [9, 10] on the basis of steady state polarization and a.c. impedance measurements. McFarlane and Smedley [11] proposed a mechanism for the process in chloride solutions also involving three parallel reaction ways. The latter was revised by Barcia and Mattos [12, 13] who explained within the framework of their model the behaviour of the metal in mixed (SO_4^{2-}–Cl^-) solutions. Recently, in two consecutive papers [14, 15], on the basis of steady state and impedance experiments the present authors proposed a model for the transpassive dissolution of pure Mo in sulphate solutions (pH 0–3) including four intermediate species in two parallel reaction paths.

A natural step towards the understanding of the mechanism of corrosion of stainless steels is the study of the various compositions of binary alloys of the steel constituents. There is a considerable amount of electrochemical data on Fe–Cr alloys. Keddam *et al.* [16, 17] proposed a quantitative model for the anodic dissolution of Fe–Cr (up to 12%) alloys in sulphate media in which interaction between iron and chromium intermediate species resulted in blocking the prepassive dissolution path of Fe. Further contributions to this binary system are due to Dobbelaar *et al.* [18, 19] in the passivation region and Annergren *et al.* [20], who used a.c. impedance in combination with a.c. RRDE measurements to assess both the active and active-to-passive range of the alloys.

On the other hand, investigations of binary Fe–Mo alloys are very scarce [21–23]. Sugimoto and Sawada [21] found that Fe–(4–20) wt % Mo alloys do not passivate in HCl but exhibit passivation features in H_2SO_4, the passive current density being the greater the higher the Mo content in the alloy. Both XPS [22, 23] and Raman spectroscopy [23] were employed to determine the composition of the passive film on binary Fe–Mo alloys and no enrichment of the latter in Mo was unambiguously observed. Little or no attention was paid to the processes of active dissolution of the alloy.

0021-891X © 1996 Chapman & Hall

In this connection, the main purposes of the present paper are as follows:
(i) To perform an experimental investigation of the active dissolution of binary Fe–Mo alloys in H_2SO_4 and HCl solutions using steady state polarization and a.c. impedance measurements.
(ii) To make a comparison between the anodic behaviour of pure Fe and the alloys in both studied media.
(iii) To elaborate a quantitative model for the anodic dissolution kinetics based on the obtained results and data from the literature concerning the anodic behaviour of pure metal constituents.

2. Experimental details

2.1. *Electrodes and electrolytes*

Iron–molybdenum alloys (10 and 20 wt % Mo) were produced by mixing spectroscopically pure Fe (Johnson Matthey) and 99.9% Mo (Koch Laboratories) in a levitation furnace under argon flow using a non-crucible method. No subsequent thermal treatment was applied. The samples were cylindrical in form and were sealed in Teflon holders by acid resistant epoxy resin in order to expose to the electrolyte a disc area of 0.072 cm^2. The electrode pretreatment consisted of mechanical polishing with emery paper grade 800 followed by a soft cloth with 50μm alumina as a grinding paste, degreasing with acetone and rinsing with distilled water. A cathodic polarization with 5 mA cm^{-2} in the experimental cell was used to remove the native film thereby formed. A conventional three-electrode cell featuring a platinized Pt counter electrode was used. In H_2SO_4 medium, a saturated mercurous sulphate electrode (SSE, $E_{NHE} = 0.670$ V) was employed as a reference whereas in HCl solutions a saturated calomel electrode (SCE) was used. The potentials in the paper are given against these two kinds of reference electrodes. The electrolytes were prepared from p.a. H_2SO_4 and HCl (Merck) and bidistilled water. The measurements were taken at room temperature (20 ± 1°C) in naturally aerated solutions (no influence of nitrogen purging on the results was detected during preliminary work).

2.2. *Apparatus and procedure*

Polarization curves were traced potentiostatically using a M273 potentiostat (Princeton Applied Research). At each potential the current–time curve was recorded until a steady state was reached. This procedure took several hours, especially at low overpotentials. No influence of stirring the solution on the values of the current was observed. All the potential values were IR drop corrected. A.c. impedance spectra were obtained at this steady state by a 5301 lock-in amplifier (Princeton Applied Research) and in the low-frequency region by a fast Fourier transform technique. The frequency range was typically between 0.03 Hz and 100 kHz at an a.c. signal amplitude of 10 mV peak-to-peak. The reproducibility of the impedance spectra was ±2% in amplitude and ±3° in phase shift. The software for data processing and impedance simulation was designed in house.

3. Results

3.1. *Polarization curves*

The steady state polarization curves of Fe and the Fe–10 wt % Mo, Fe–20 wt % Mo alloys in 1 M H_2SO_4 are presented in Fig. 1, and for 1 M HCl in Fig. 2.

The curves for pure iron are in quantitative agreement with those published by Keddam *et al.* [9] in sulphate solutions and McFarlane and Smedley [11] in chloride, bearing in mind the higher chloride concentration (4 M) used by the latter authors. The Figures

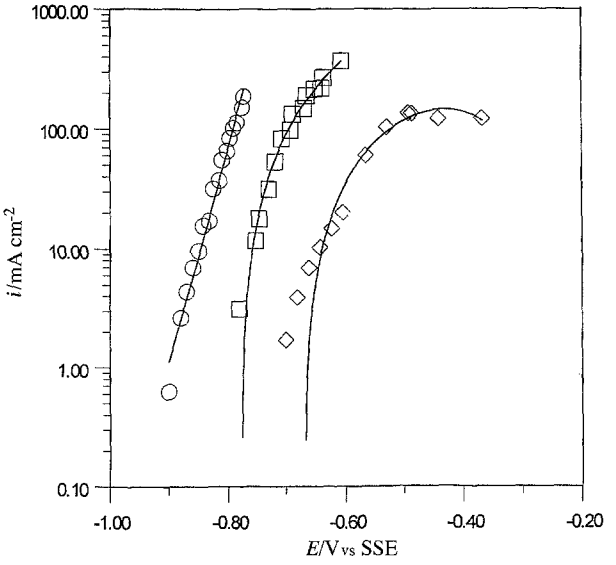

Fig. 1. Steady state polarization curves of the active dissolution of pure Fe (○), Fe–10% Mo (□) and Fe–20% Mo (◇) alloys in 1 M H_2SO_4.

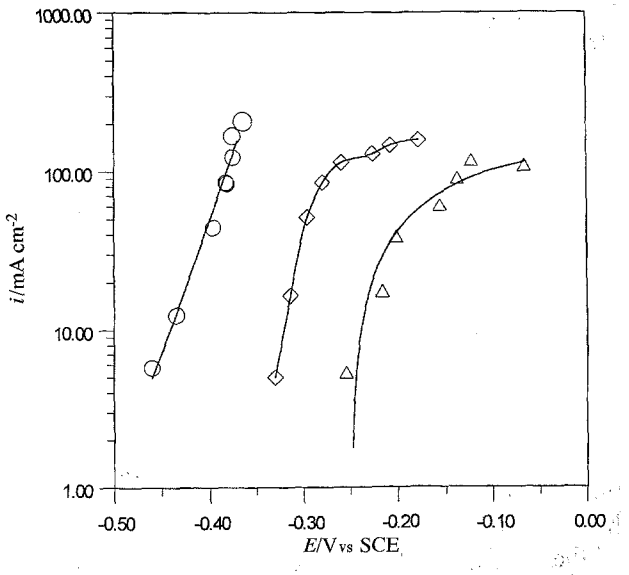

Fig. 2. Steady state polarization curves of the active dissolution of pure Fe (○), Fe–10% Mo (◇) and Fe–20% Mo (△) alloys in 1 M HCl.

show that the rest potential is shifted towards more positive values with the addition of Mo (Figs 1 and 2). The influence of molybdenum additive on the value of the current is clear, especially in the high overpotential region, where a significant curvature of the polarization curve is observed in comparison to pure iron (Figs 1 and 2). This feature is more pronounced for the Fe–20% Mo alloy, exhibiting a maximum at very high overpotentials. The main conclusion is that molybdenum additive significantly alters the d.c. polarization behaviour of iron in the active dissolution region, this effect being the stronger the higher the molybdenum content in the alloy.

3.2. *A.c. impedance spectra*

A.c. impedance spectra for pure iron in the two media under study are presented in Fig. 3 (Fe, 1 M H_2SO_4) and Fig. 4 (Fe, 1 M HCl).

The data are in qualitative agreement with that published in [9, 11, 12]. Some quantitative differences are observed which may be due to the origin of the iron samples and their thermal pretreatment. In general, regardless of the medium, two pseudo-inductive loops are always observed besides the charge transfer semicircle, implying the existence of at least two reaction intermediates.

The impact of Mo additive on the impedance

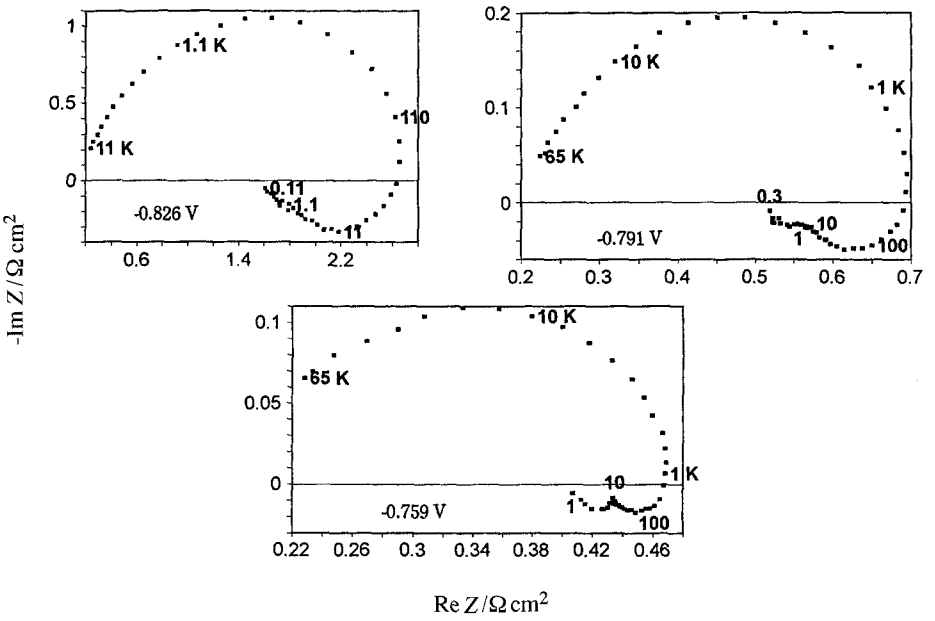

Fig. 3. A.c. impedance spectra of the active dissolution of spectroscopically pure Fe (15 ppm impurities) in 1 M H_2SO_4. Parameter is frequency in hertz.

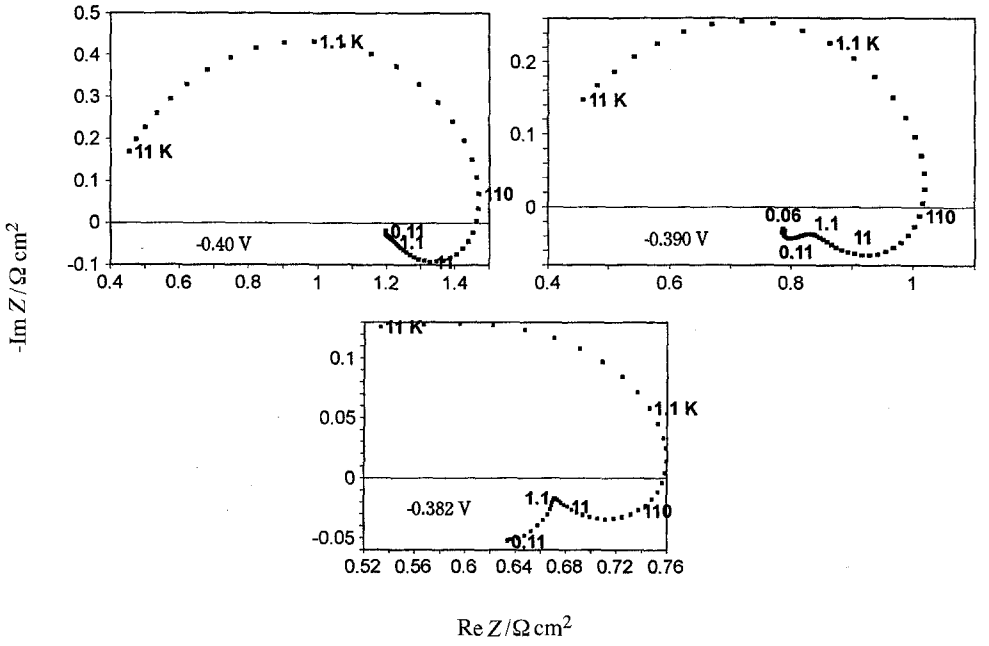

Fig. 4. A.c. impedance spectra of the active dissolution of spectroscopically pure Fe (15 ppm impurities) in 1 M HCl. Parameter is frequency in hertz.

spectra of iron in 1 M H_2SO_4 is depicted in Figs 5 (Fe–10% Mo alloy) and 6 (Fe–20% Mo alloy).

For low overpotentials, the spectra for Fe–10% Mo are qualitatively similar to those of pure iron (cf. Figs 3 and 5). At high overpotentials, however, the medium frequency inductive loop becomes capacitive and for still higher ones the beginning of another loop in the lowest frequency range is detected (Fig. 5). For the Fe–20% Mo alloy, no 'iron-like' region is observed (cf. Figs 3 and 6) and the spectra in the whole studied range are qualitatively similar to those for Fe–10% Mo in the high overpotential region (cf. Figs 5 and 6). For overpotentials greater than the current maximum in Fig. 1, a passivation process is detected (last spectrum in Fig. 6). A gold coloured film is formed on the Fe–20% Mo surface at these potentials which is loosely adherent and spalls from the electrode. Chemical analysis of the solution suggested the formation of sparingly soluble Mo(VI) species such as the yellow-brown $MoO_3 \cdot 2H_2O$. Thus, passivation may be associated with the formation of this film. A study of the process will be attempted in further work.

The impact of Mo additive on the impedance spectra of iron in 1 M HCl is illustrated in Fig. 7 (Fe–10% Mo alloy) and Fig. 8 (Fe–20% Mo alloy).

In hydrochloric acid solution, molybdenum additive action leads to the transformation of the lowest frequency pseudo-inductive loop into a capacitive one (cf. Fig. 4 and Figs 7 and 8), the effect being qualitatively similar for both Mo contents (cf. Figs 7 and 8). No passivation features were observed either in the

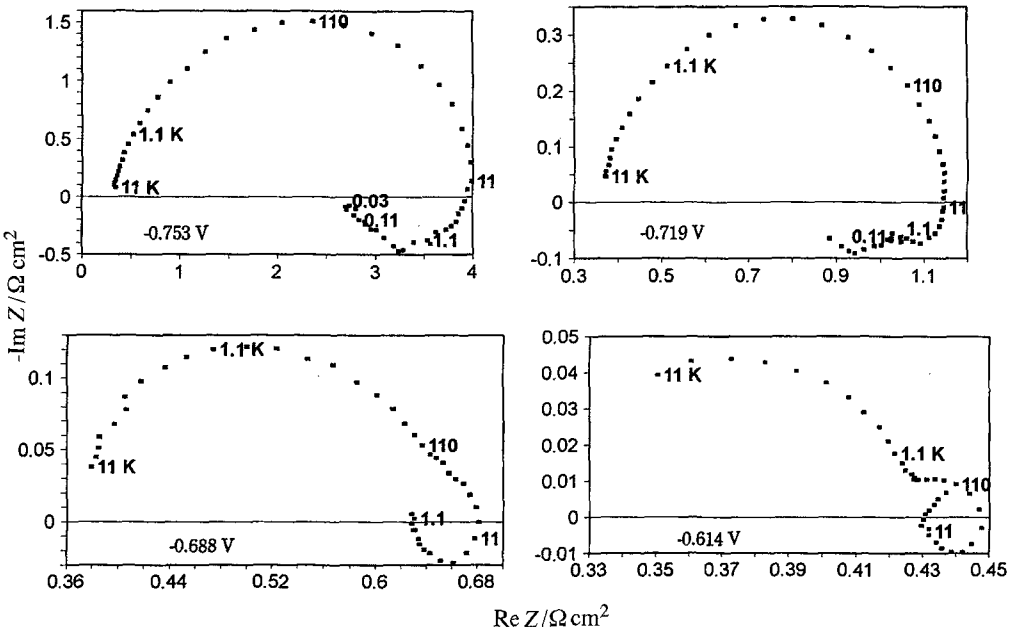

Fig. 5. A.c. impedance spectra of the active dissolution of a Fe–10% Mo alloy in 1 M H_2SO_4. Parameter is frequency in hertz.

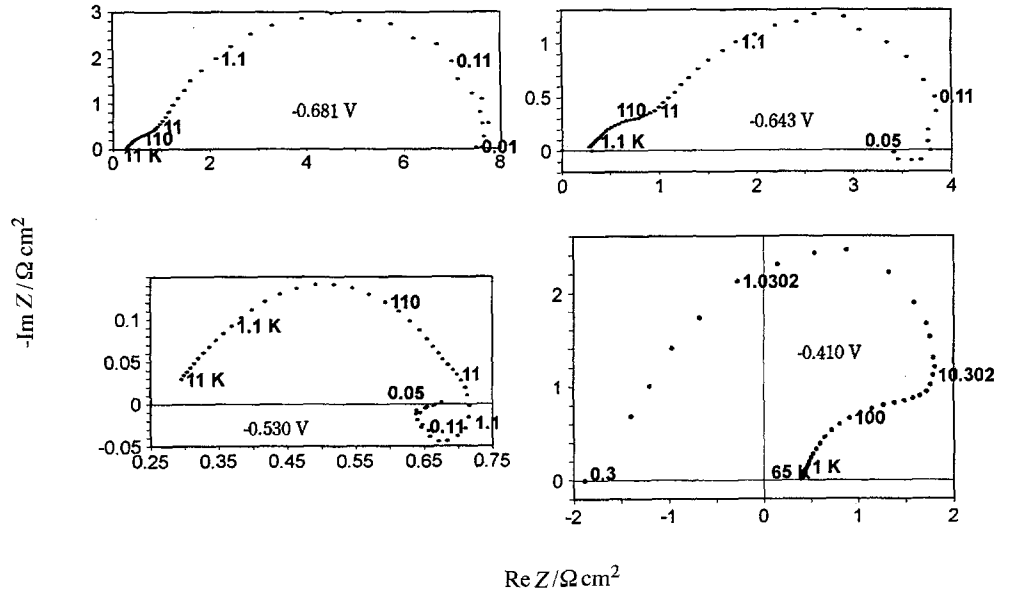

Fig. 6. A.c. impedance spectra of the active dissolution of a Fe–20% Mo alloy in 1 M H_2SO_4. Parameter is frequency in hertz.

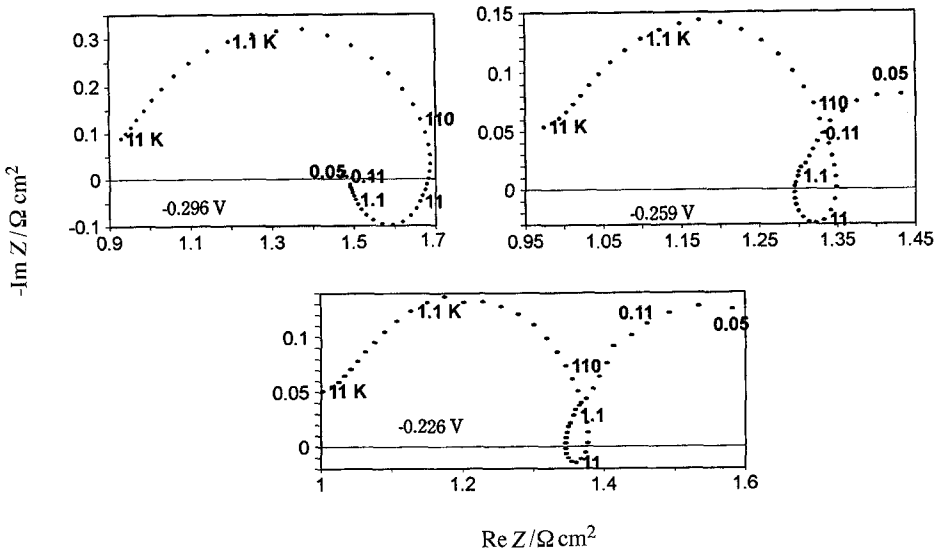

Fig. 7. A.c. impedance spectra of the active dissolution of a Fe–10% Mo alloy in 1 M HCl. Parameter is frequency in hertz.

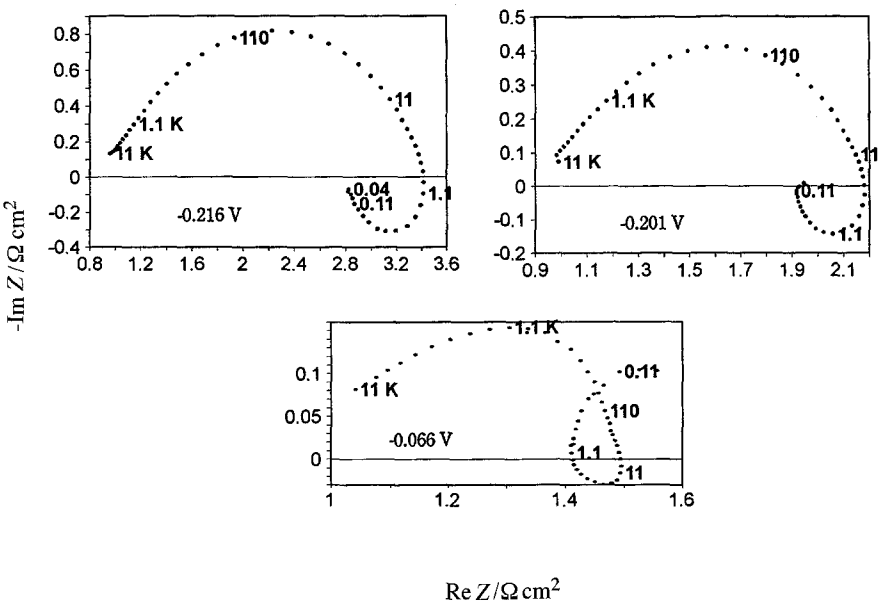

Fig. 8. A.c. impedance spectra of the active dissolution of a Fe–20% Mo alloy in 1 M HCl. Parameter is frequency in hertz.

polarization curves or in the impedance spectra in HCl. In the low overpotential region, the spectra for Fe–10% Mo alloy are qualitatively similar to those for Fe, whereas the two inductive loops overlap for Fe–20% Mo.

It can be concluded that molybdenum additive modifies the mechanism of active dissolution of iron both in H_2SO_4 and HCl media. In H_2SO_4 medium, Mo acts to transform the medium frequency loop from inductive to capacitive, whereas in HCl medium Mo action is confined to such a transformation of the lowest frequency loop. Thus Mo addition favours different reaction paths and influences the stability of the dissolution intermediates in the two media.

4. Discussion

The mechanism of anodic dissolution of iron in H_2SO_4 solution was elucidated by impedance techniques in the work of Keddam *et al.* [9, 10], whereas in HCl solutions mechanisms were proposed by McFarlane and Smedley [11] and Barcia and Mattos [12, 13]. Very recently, we proposed a model for the transpassive dissolution of Mo in H_2SO_4 [14, 15]. No active dissolution of Mo was observed, in accordance with earlier work. Thus, models for iron dissolution must be used as a basis of the explanation of the behaviour of Fe–Mo alloys. The model used here is very similar to those advanced for pure iron in H_2SO_4 and HCl solutions. It can be depicted as follows:

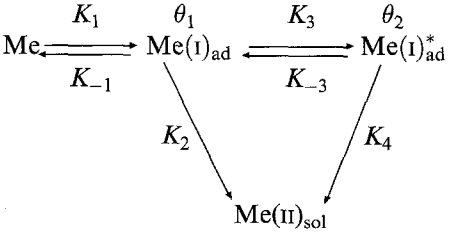

where the K_4 step is a catalytic process of the type suggested by Keddam *et al.* [9, 10]

$$Me(I)^*_{ad} + Me \rightarrow Me(II)_{sol} + Me(I)^*_{ad} + 2e^-$$

So far, the symbol 'Me' is used instead of individualizing the dissolution of Fe and Mo surface positions in the film. Thus, within the framework of the present approach, the alloy electrode is regarded as a continuous uniformly dissolving surface and the rate constants are defined as mean values over the whole electrode area.

The classical assumption of Langmuir adsorption and Tafel dependence of the reaction rate constants [10]

$$K_i = K_i^o \exp(\pm b_i E), \quad i = 1, 2, 3, 4, -1, -3$$

where E is the overpotential expressed against the rest potential of the alloy electrodes in both media, leads to the following balances at the interface:

Charge balance

$$I = F[K_1(1 - \theta_1 - \theta_2) - (K_{-1} - K_2)\theta_1 + 2K_4\theta_2] \quad (1)$$

Mass balances of the intermediates

$$\beta \, d\theta_1/dt = K_1(1 - \theta_1 - \theta_2) - (K_{-1} + K_2 + K_3)\theta_1 + K_{-3}\theta_2 \quad (2)$$

$$\beta \, d\theta_2/dt = K_3\theta_1 - K_{-3}\theta_2 \quad (3)$$

The steady-state solution can be obtained by setting the above time derivatives to zero:

$$\theta_{1s} = K_1K_{-3}/D \quad (4)$$

$$\theta_{2s} = K_1K_3/D \quad (5)$$

$$D = K_1K_3 + K_{-1}K_{-3} + K_2K_{-3} + K_1K_{-3}$$

$$I = 2F\{K_2\theta_{1s} + K_4\theta_{2s}\} \quad (6)$$

The faradaic impedance is derived from a Taylor expansion of Equations 1 to 3 to the first order

$$Z_F^{-1} = R_t^{-1} - F[(K_1 + K_{-1} - K_2)d\theta_1/dE + (K_1 - 2K_4)d\theta_2/dE] \quad (7)$$

where

$$R_t^{-1} = F\{[(b_1 - b_{-1})K_{-1} + (b_1 + b_2)K_2]\theta_{1s} + 2b_4K_4\theta_{2s}\} \quad (8)$$

$$d\theta_1/dE = [A_1Z_2 - (K_1 - K_{-3})A_2]/Z_D$$

$$d\theta_2/dE = [A_2Z_1 + A_1K_3]/Z_D$$

$$A_1 = [(b_1 - b_{-1})K_{-1} + (b_1 - b_2)K_2 - (b_3 - b_{-3})K_3]\theta_{1s}$$

$$A_2 = (b_3 - b_{-3})K_{-3}]\theta_{2s}$$

$$Z_1 = K_1 + K_{-1} + K_2 + K_3 + j\omega\beta$$

$$Z_2 = K_{-3} + j\omega\beta$$

$$Z_D = Z_1Z_2 + (K_1 - K_{-3})K_3$$

To obtain the total interfacial impedance, the double layer capacitance, C_d, (assumed to be potential independent for the sake of simplicity) and the electrolyte resistance, R_{el}, have to be appropriately added to the faradaic impedance.

$$Z = (Z_F^{-1} + j\omega C_d)^{-1} + R_{el} \quad (9)$$

The ability of the proposed model to reproduce the steady state polarization curves and impedance spectra is demonstrated in Fig. 9 (Fe–20% Mo, 1 M H_2SO_4) and 10 (Fe–10% Mo, 1 M HCl). The potential

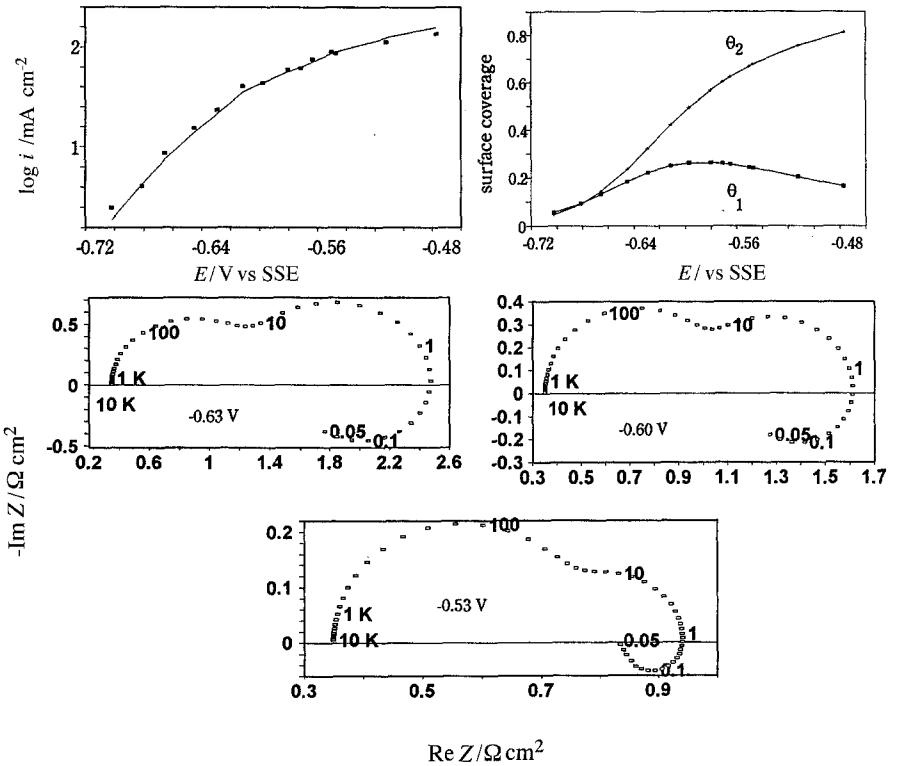

Fig. 9. Experimental (points) against simulated (solid line) steady state polarization curves and simulated a.c. impedance spectra for a Fe–20% Mo alloy in 1 M H_2SO_4. Parameter is frequency in hertz.

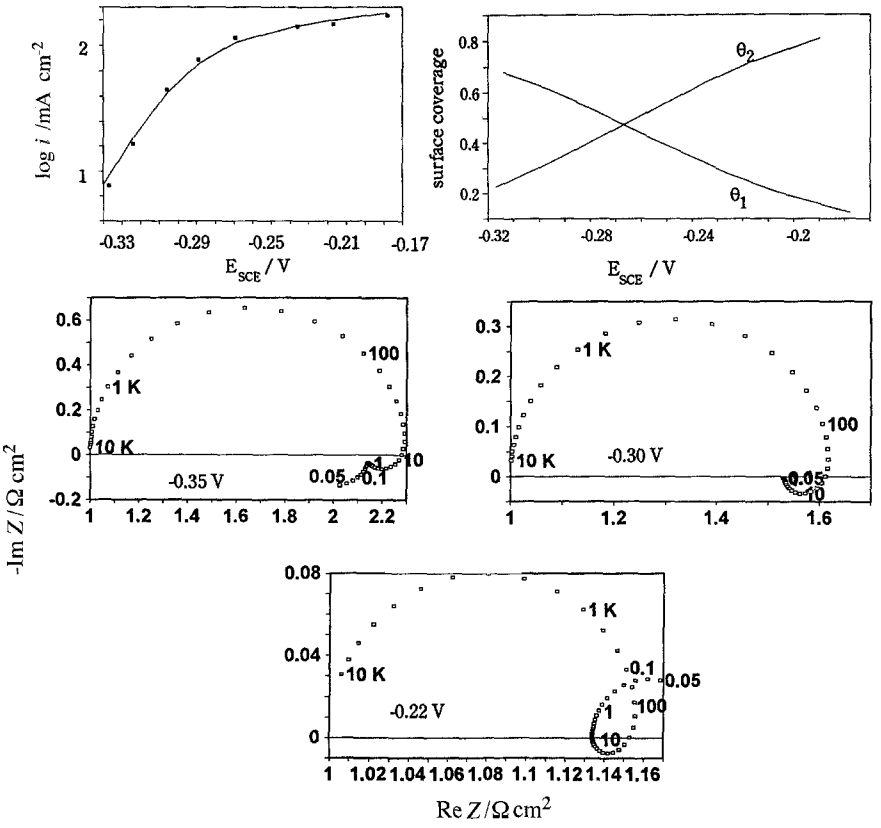

Fig. 10. Experimental (points) against simulated (solid line) steady state polarization curves and simulated a.c. impedance spectra for a Fe–10% Mo alloy in 1 M HCl. Parameter is frequency in hertz.

dependence of the steady state surface coverages θ_{1s} and θ_{2s} is also shown in the Figures. The values of the model parameters for both alloys in the two media are summarized in Table 1.

No fitting procedure was used, but the parameter values were adjusted manually to give the closest possible matching of the experimental results. However, the existence of another set of kinetic parameters ensuring equally good or even better fit to the experimental data cannot be excluded. Thus the values of the kinetic constants should be regarded as a first estimation of the real parameters.

A comparison between Figs 6 and 9, 7 and 10, respectively, demonstrates that both the values of the impedance and its frequency distribution are successfully simulated, together with the steady state current density. The main discrepancies lay in the fact that with one and the same set of parameters, it was impossible to obtain diameters of all the three loops matching the experimental ones sufficiently closely. The use of a fitting procedure would certainly achieve better coincidence, but with the huge number of adjustable parameters the probability for an optimization procedure to converge in a local extremum is very

Table 1. Kinetic parameters of the proposed model used to simulate both the steady state polarization curves and the a.c. impedance diagrams (Figs 9 and 10) for the Fe–10% Mo and Fe–20% Mo alloys in 1 M H_2SO_4 and HCl

Kinetic parameters	*Fe–10% Mo /1 M H_2SO_4*	*Fe–20% Mo /1 M H_2SO_4*	*Fe–10% Mo /1 M HCl*	*Fe–20% Mo /1 M HCl*
K_1^0/mol cm^{-2} s^{-1}	1×10^{-8}	4×10^{-8}	4×10^{-7}	3×10^{-7}
K_{-1}^0/mol cm^{-2} s^{-1}	2×10^{-6}	2×10^{-6}	2×10^{-7}	7×10^{-8}
K_2^0/mol cm^{-2} s^{-1}	8×10^{-9}	5×10^{-8}	1×10^{-8}	2×10^{-8}
K_3^0/mol cm^{-2} s^{-1}	3×10^{-9}	6×10^{-9}	1×10^{-9}	1×10^{-9}
K_{-3}^0/mol cm^{-2} s^{-1}	1×10^{-8}	8×10^{-9}	2×10^{-8}	3×10^{-8}
K_4^0/mol cm^{-2} s^{-1}	3×10^{-7}	1×10^{-7}	5×10^{-7}	4×10^{-7}
b_1/V^{-1}	36	26	18	18
b_{-1}/V^{-1}	12	5	12	10
b_2/V^{-1}	31	17	32	31
b_3/V^{-1}	5	3	22	20
b_{-3}/V^{-1}	2	2	0	0
b_4/V^{-1}	8	7	5	3
β/mol cm^{-2}	2×10^{-8}	4×10^{-8}	4×10^{-8}	3×10^{-8}
C_d/μF cm^{-2}	1000	3000	200	300

large; thus we preferred the simpler simulation approach.

The values of the kinetic constants listed in Table 1 enable several tentative suggestions on the influence of Mo concentration and anion type on the mechanism of the anodic dissolution to be made:

(i) The standard rate constants of the irreversible dissolution steps 2 and 4 are weakly influenced by both Mo content and anion type, but the Tafel coefficient of step 2 is significantly higher in Cl^- solutions, whereas that of step 4 is significantly lower in the same medium when compared with H_2SO_4 solution.

(ii) The influence of Mo content over the kinetic parameters in HCl solutions is less pronounced than in H_2SO_4.

(iii) The reverse reactions of steps 1 and 3 are more strongly influenced by both Mo content and anion type than is the forward reaction. Thus, it can be concluded that the reaction steps in the proposed model are not true elementary steps, but merely depict the detectable stages of the overall process by the electrochemical methods used in the present work (see also [24]). This suggestion is supported by the fact that $b_i \neq b_{-i}$ for all the quasi-reversible steps [24]. In principle it is possible to postulate a sequence of true elementary steps for the dissolution of the alloy and to suggest a possible role of Mo at atomic level, but such hypotheses will remain highly speculative if based only on purely electrochemical techniques which do not provide information on the chemical nature of species involved.

(iv) The values of β are practically not sensitive to both Mo content and the electrolyte type, being 2–4 times greater than those usually postulated for active dissolution of a metal [16]. This fact, together with the obtained value of the sum $\theta_{1s} + \theta_{2s} \approx 1$ (Figs 9 and 10), suggests that a very thin conductive layer is present on the electrode surface. This is in accordance with the results on pure Mo [14, 15] and could also explain the relatively high values of the apparent double layer capacitance, especially in H_2SO_4 medium (Table 1).

5. Conclusions

The anodic behaviour of Fe–Mo alloys (10 and 20 wt % Mo) in 1 M H_2SO_4 and HCl was investigated by steady state polarization and a.c. impedance techniques, emphasizing active dissolution. A quantitative model of the interface is advanced based on literature data for iron dissolution in the studied media. It was possible to reproduce the general features of the impedance spectra and steady state polarization curves. As a conclusion, several points needing further clarification will be emphasized and the limitations of the model will be outlined.

(i) No quantitative expression for the influence of Mo on the anodic dissolution kinetics analogous to that proposed by Keddam *et al.* [16, 17] could be advanced. Rather, the proposed model is a global one neglecting the individualities of the surface metal positions. In this connection, the calculated parameters represent mean values with the alloy surface treated as homogeneously dissolving. Further studies using surface analytical methods are needed in order to clarify the role of Mo in altering the anodic dissolution kinetics.

(ii) The passivation process taking place at higher Mo content in H_2SO_4 solution involving the formation of an unstable Mo(VI) film needs further investigation. It was not taken into account within the framework of the proposed approach. In general, the passive state of the alloys must be less stable than for pure Fe due to the transpassive dissolution of Mo. Further studies in media enabling pure Mo passivation via the formation of a stable anodic film are in progress which will help to characterize the influence of Mo on the passive dissolution of Fe.

Acknowledgements

The financial support of the National Scientific Research Fund, Bulgarian Ministry of Science, Education and Technologies under contract CH-330 is gratefully acknowledged. The authors are indebted to Prof. Tz. Rashev from the Institute of Metal Science, Bulgarian Academy of Sciences for the preparation of the alloy samples.

References

[1] C. Chao, L. Lin and D. D. Macdonald, *J. Electrochem. Soc.* **128** (1981) 1187.
[2] *Idem, ibid.* **128** (1981) 1194.
[3] *Idem, ibid.* **129** (1982) 1874.
[4] D. D. Macdonald and M. Urquidi-Macdonald, *ibid.* **137** (1990) 2395.
[5] D. D. Macdonald and S. I. Smedley, *Electrochim. Acta* **35** (1990) 1949.
[6] D. D. Macdonald, *J. Electrochem. Soc.* **139** (1992) 3434.
[7] M. Urquidi and D. D. Macdonald, *ibid.* **132** (1985) 555.
[8] M. Urquidi-Macdonald and D. D. Macdonald, *ibid.* **136** (1989) 961.
[9] M. Keddam, O. R. Mattos and H. Takenouti, *ibid.* **128** (1981) 257.
[10] *Idem, ibid.* **128** (1981) 266.
[11] D. R. MacFarlane and S. I. Smedley, *ibid.* **133** (1986) 2240.
[12] O. E. Barcia and O. R. Mattos, *Electrochim. Acta* **35** (1990) 1003.
[13] *Idem, ibid.* **35** (1990) 1601.
[14] M. Bojinov, I. Betova and R. Raicheff, *J. Electroanal. Chem.* **381** (1995) 123.
[15] *Idem, Electrochim. Acta*, in press.
[16] M. Keddam, O. R. Mattos and H. Takenouti, *Electrochim. Acta.* **31** (1986) 1147.
[17] *Idem, ibid.* **31** (1986) 1159.
[18] J. A. L. Dobbelaar, E. C. M. Herman and J. H. W. de Wit, *Corros. Sci.* **33** (1992) 765.
[19] *Idem, ibid.* **33** (1992) 779.
[20] I. Annergren, M. Keddam, H. Takenouti and D. Thierry, *Electrochim. Acta* **38** (1993) 763.
[21] K. Sugimoto and Y. Sawada, *Corros. Sci.* **17** (1977) 425.
[22] K. Hashimoto, M. Naka, K. Asami and T. Masumoto, *ibid.* **19** (1979) 165.
[23] D. Thierry, D. Persson, C. Leygraf, N. Boucherit and A. Hugot-le-Goff, *Corros. Sci.* **32** (1991) 273.
[24] M. Keddam, H. Takenouti and N. Yu, *J. Electrochem. Soc.* **132** (1985) 2561.